Kinetic study and Box–Behnken design approach to optimize the sorption process of toxic azo dye onto organo-modified bentonite

Brahim Guezzen, Mehdi Adjdir, Baghdad Medjahed, Mohamed A. Didi, and Peter G. Weidler

Abstract: Kinetic study was applied for sodium bentonite (Na-B) and hexadecylpyridinium bentonite (HDP-B) under different amounts, namely 50% (50HDP-B), 100% (100HDP-B), and 200% (200HDP-B) with respect to cation exchange capacity (CEC). Pseudo first-order and pseudo second-order kinetic models were performed to optimize the sorption of Congo red (CR) dye from aqueous solution. The experimental data fit the pseudo second order kinetic model well. The sorption capacity (q_e) of CR dye by the organo-bentonites at equilibrium was 36.0 mg g^{-1} (72.1%) for 50HDP-B, 48.05 mg g^{-1} (96.1%) for 100HDP-B, and 49.2 mg g^{-1} (98.4%) for 200HDP-B. These results were considerably higher than that found by Na-B. Response surface methodology with three-variable, three-level Box–Behnken design was applied for 100HDP-B to describe the removal of CR dye. The effects of three variables, namely temperature, adsorbent dosage, and initial dye concentration, were studied. Predicted values of adsorption efficiency were found to be in good agreement with the obtained experimental values (R^2 = 0.97). A second-order polynomial model successfully described the effects of independent variables on the CR dye removal. At the optimized condition, the toxic azo dye could be quantitatively removed from aqueous solution. The results of the present study suggest that the organo-bentonite can be used as an efficient sorbent for dye removal from aqueous solution.

Key words: organo-bentonite, Congo red dye, kinetics study, Box–Behnken design.

Résumé : Nous avons mené une étude cinétique sur la bentonite sodique (Na-B) et des bentonites modifiées par l'hexadécylpyridinium (HDP-B) de différentes compositions, soit 50 % (50HDP-B), 100 % (100HDP-B) et 200 % (200HDP-B), afin d'examiner leur capacité d'échange cationique (CEC). Nous avons utilisé les modèles cinétiques de pseudo-premier ordre et de pseudo-second ordre pour optimiser la sorption du colorant azoïque rouge Congo (RC) en solution aqueuse. Les données expérimentales concordaient très bien avec le modèle cinétique de pseudo-second ordre. La capacité de sorption (q_e) du RC par les organobentonites à l'équilibre était de 36,0 mg g^{-1} (72,1 %) pour la 50HDP-B, de 48,05 mg g^{-1} (96,1 %) pour la 100HDP-B et de 49,2 mg g^{-1} (98,4 %) pour la 200HDP-B. Ces résultats étaient considérablement plus élevés que ceux observés pour la Na-B. Nous avons appliqué la méthode des surfaces de réponse couplée à un plan de Box-Behnken à trois facteurs et à trois niveaux pour décrire l'élimination du colorant RC par la 100HDP-B. Pour ce faire, nous avons étudié les effets de trois variables, soit la température, la quantité d'adsorbant et la concentration initiale de colorant. Nous avons constaté une bonne concordance entre les valeurs calculées de l'efficacité d'adsorption et les valeurs expérimentales (R^2 = 0,97). Un modèle polynomial de second ordre permet de décrire adéquatement les effets des variables indépendantes sur l'élimination du colorant RC. En conditions optimisées, ce colorant azoïque toxique peut être éliminé quantitativement d'une solution aqueuse. Les résultats de la présente étude permettent de penser que cette organobentonite peut être utilisée comme sorbant pour l'élimination efficace de colorants en solutions aqueuses. [Traduit par la Rédaction]

Mots-clés : organobentonite, colorant rouge Congo, étude cinétique, méthode de Box–Behnken.

Introduction

The use of synthetic dyes in the food, pharmaceutical, cosmetics, textiles, paper, dyeing, and plastics industry has been growing since the beginning of the century, favoring the emergence of numerous clinical manifestations. World production is estimated at 700 000 tonnes $year^{-1}$, of which 140 000 tonnes are discharged into the effluents during different stages of application and confection.[1,2] Azo-compounds are the most important family in terms of application, accounting for more than one-half of the dyes prepared worldwide. These structures are characterized by the azo (–N=N–) functional group uniting two identical or different alkyl or aryl radicals.[3,4] This dye category is currently the most widely used in terms of application, accounting for more than 50% of global dye production.[5,6] It is estimated that 10%–15% of the initial quantities are lost during dyeing procedures and are discharged without prior treatment in the effluents.[6] The azo bond is the most labile portion of these molecules and can easily break

B. Guezzen and B. Medjahed. Laboratory of Separation and Purification Technology, Department of Chemistry, Faculty of Sciences, Tlemcen University, Box 119, Algeria; Department of Process Engineering, Faculty of Technology, Dr. Moulay Tahar University, Saida, Algeria.
M. Adjdir. Department of Process Engineering, Faculty of Technology, Dr. Moulay Tahar University, Saida, Algeria; Chemistry of Oxydic and Organic Interfaces, Karlsruher Institut für Technologie (KIT)/Campus Nord, Hermann-von-Helmholtz-Platz 1, Germany.
M.A. Didi. Laboratory of Separation and Purification Technology, Department of Chemistry, Faculty of Sciences, Tlemcen University, Box 119, Algeria.
P.G. Weidler. Chemistry of Oxydic and Organic Interfaces, Karlsruher Institut für Technologie (KIT)/Campus Nord, Hermann-von-Helmholtz-Platz 1, Germany.

Corresponding authors: Brahim Guezzen (email: b_guezzen@yahoo.fr) and Mehdi Adjdir (email: mehdi.adjdir@daad-alumni.de).

Scheme 1. (*a*) Structure of CR dye and the (*b*) structure of HDPCl.

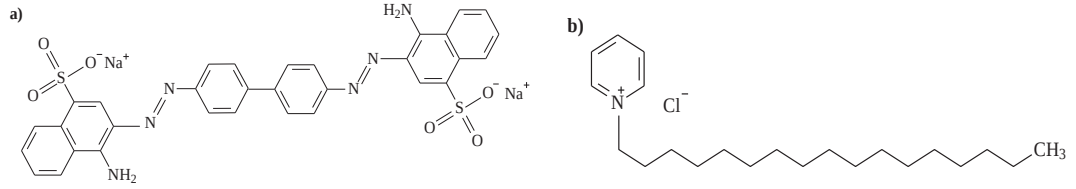

under the enzymatic action of mammalian organisms, including humans, to become a carcinogenic amino compound.[7,8] These carcinogenic organic compounds are resistant to treatment and biodegradation.[9]

To remove dye contaminants that damage the ecosystem and water supply (used for drinking water supply, water industry needs, agriculture, etc.), numerous processes are implemented, including adsorption,[10] ozonation,[11] coagulation/flocculation,[12] membrane separation,[13] advanced oxidation processes,[14,15] and biological treatment.[16,17] Adsorption has been recognized as the most popular treatment process for dye removal in aqueous solution and has the advantages of high efficiency, simple operation, and easy recovery and reuse of adsorbent.[18] In the current work, Congo red (CR) dye was selected as the target molecule for adsorption because this molecule is the subject of many other studies on the removal of azo dye pollutants.[19–21] Various reports have shown that organo-modified clays are cost-effective in the sorption of several contaminants as a result of being hydrophobic and organophilic, readily available, and environmentally stable. The present paper reports the preparation of hexadecylpyridinium intercalated clay from the natural bentonite of Maghnia, northwestern Algeria. The investigation focuses on the use of modified clay and the adsorption kinetics and optimization process of CR dye from aqueous solutions. An attempt is also made to optimize the process parameters such as temperature, adsorbent dosage, and initial dye concentration using statistical experiment design based on the Box–Behnken matrix to study the linear, square, and interactive effects of process parameters on the removal of CR dye from aqueous solution by a selected organo-bentonite sample.

Materials and methods

Chemicals and reagents

The sample clay used in this study came from Maghnia with a mineralogical composition of about 80 wt.% montmorillonite, 10% quartz, 3.0% cristobalite, and less than 1% beidellite. Its chemical composition was as follows: 62.48% SiO_2, 17.53% Al_2O_3, 1.23% Fe_2O_3, 3.59% MgO, 0.82% K_2O, 0.87% CaO, 0.22% TiO_2, 0.39% Na_2O, and 0.04% As, with 13.0% loss on ignition at 950 °C.[22]

The surfactant hexadecylpyridinium chloride monohydrate HDPCl ($C_{21}H_{40}ClNO$) (purity of > 99%) and the CR dye ($C_{32}H_{22}N_6Na_2O_6S_2$) (purity of >99%) were purchased from Biochem. The chemical structures of the CR and HDPCl are given in Scheme 1.

Preparation of HDP-B samples and characterization methods

The natural bentonite used in this study was processed to < 2 μm size fraction by sedimentation in deionized water. It was purified and converted to sodium bentonite (Na-B), using the method described by Makhoukhi et al.[23] The cation exchange capacity (CEC) of sodium bentonite was calculated by using the methylene blue adsorption method[24] and was found to be 93 meq/100 g.

HDP-intercalated bentonite samples were prepared by intercalation of the pyridinium cation into the Na-B suspension following a previously described procedure.[25] Briefly, 25 g of the samples was mixed with 500 mL of cationic surfactant HDPCl solutions with various amounts corresponding to 50%, 100%, and 200% of the CEC of the Na-B. The mixture was agitated for 24 h at room temperature and then centrifuged at 3000 rpm for 15 min. Next, the suspension was filtered, washed several times with distilled water (until negative chloride test with 0.1 mol/L $AgNO_3$ was obtained), and dried at 70 °C for 24 h. The materials obtained were designated as 50HDP-B, 100HDP-B, and 200HDP-B.

The HDP-B samples were compared with Na-B with Fourier transform infrared (FTIR) spectroscopy. Infrared spectra were recorded over the range 4000–500 cm^{-1} with a Perkin Elmer FTIR spectrophotometer.

Adsorption procedure

A stock solution of the CR dye with a concentration of 1000 mg L^{-1} was prepared in distilled water. From the stock solution, various concentrations were prepared by dilution. In kinetic studies, batch adsorption experiments were carried out in a 100 mL Erlenmeyer flask by adding 25 mg of sorbent to 25 mL CR solution (50 mg L^{-1}) at a natural pH of 6.6 and a room temperature of 20 ± 1 °C on a thermostatic shaker with a shaking speed of 250 rpm. The samples were withdrawn at different times until 180 min. The suspensions were then centrifuged and analyzed using Analytik Jena SPECORD 210 Double Beam UV–vis spectrophotometer at λ_{max} = 498 nm. The amount (mg) of dye adsorbed per gram of adsorbent at the time t (q_t), the adsorption capacity (mg g^{-1}) at equilibrium (q_e) and percent removal (% removal) were calculated using the following equations:

$$q_t = (C_0 - C_t)\frac{V}{m} \quad (1)$$

$$q_e = (C_0 - C_e)\frac{V}{m} \quad (2)$$

$$\%\ \text{removal} = \left(1 - \frac{C_t}{C_0}\right)100 \quad (3)$$

where C_0 (mg L^{-1}) and C_e (mg L^{-1}) are the initial and equilibrium concentrations of CR dye, respectively, m (g) is the amount of adsorbent, and V (L) is the volume of the aqueous solution.

Two types of kinetic models were used to test the experimental data of the adsorption of CR dye onto organoclays: pseudo first-order equation[26] and pseudo second-order equation models.[27] These models can be expressed in an integrated and linearized form using the following equations:

$$\log(q_e - q_t) = \log q_e - \left(\frac{k_1}{2.303}\right)t \quad (4)$$

$$\frac{t}{q_t} = \frac{1}{k_2 q_e^2} + \frac{1}{q_e}t \quad (5)$$

where k_1 and k_2 are the equilibrium rate constants of pseudo first-order (min^{-1}) and pseudo second-order model (g mg^{-1} min^{-1}), respectively.

The initial sorption rate, h (mg g^{-1} min^{-1}), at $t \to 0$ is defined as

$$h = k_2 q_e^2 \quad (6)$$

Table 1. Codification and levels of the three independent variables considered for the sorption of CR dye.

	Range and levels		
Variable	Low (–1)	Medium (0)	High (+1)
Temperature, X_1 (°C)	20	40	60
Solid–solution ratio, X_2 (g L^{-1})	0.1	0.55	1
Initial dye concentration, X_3 (mg L^{-1})	50	275	500

To study the effect of temperature on the sorption capacity of dye by 100HDP-B sample, adsorption experiments were carried out with 50 mg L^{-1} of CR dye (m/V = 1 g L^{-1}) by varying the temperature (20, 40, and 60 °C).

The effects of initial dye concentration (50–500 mg L^{-1}) and solid–solution ratio (0.1–2 g L^{-1}), on the amount of adsorbed dye both on Na-B and 100HDP-B were obtained at a constant temperature of 20 ± 1 °C. The contact time was set to 120 min (equilibrium time).

Experimental design

Experimental design methods are a very powerful tool for the improvement and optimization of processes and can also be very useful in establishing statistical control of a process. Their applications can also play a major role in technical design activities, where new products are developed and existing products are improved. The operational variables such as temperature, solid–solution ratio, and initial dye concentration of the CR sorption process using 100HDP-B were optimized based on the Box–Behnken design. The percent removal of dye (Y) is selected as a response for the combination of independent variables, which is fitted by a second-order polynomial model:

$$(7) \qquad Y = \beta_0 + \sum_{i=1}^{n} \beta_i X_i + \sum_{i=1}^{n} \beta_{ii} X_i^2 + \sum_{i=1}^{n-1} \sum_{j=2}^{n} \beta_{ij} X_i X_j$$

where Y is the predicted percent removal, X_i and X_j are the input variables that affect the response, n is the number of independent variables, β_0 is a constant, and β_i, β_{ii}, and β_{ij} are the coefficients estimated from regression and represent the linear, quadratic, and cross products of variables on response, respectively. The experimental data were processed by using the Statgraphics Centurion XVI software.

A Box–Behnken design matrix with three factors and three levels was examined to not only investigate the main and interactive effects of the process variables, but also obtain the optimum operational variables for the CR dye removal. The range and level of experimental variables are shown in Table 1.

Results and discussion

FTIR spectroscopy analysis

The FTIR spectra of Na-B and the HDP-B samples are shown in Fig. 1. From the IR spectra of adsorbents, a band around 3630 cm^{-1} was attributed to the Al_2OH group of the octahedral layer.[28] The broad bands around 3420 and 1045 cm^{-1} can be associated with the overlapping symmetric and asymmetric hydroxyl group stretching vibration of water molecules on the external layer and to asymmetric stretching vibration of Si–O–Si tetrahedra in the montmorillonite, respectively.[29,30] A comparison of the FTIR spectra of HDP-B with that of Na-B exhibits significant changes in some of the peaks. The intercalation of the surfactant in the bentonite showed the role of the siloxane group resulting in the displacement of the peak from 1045 to 1024 cm^{-1}.[31] From the IR spectra of the organo-modified clay (HDP-B), the absorption bands observed at 2800–3000 cm^{-1} corresponded to –CH– stretching vibration. These bands are absent for Na-B, which shows that hexadecylpyridinium is well incorporated into the bentonite. Additionally, the band at 1474 cm^{-1} was ascribed to the aromatic C=C vibrations.[32]

Fig. 1. IR spectra of sodium bentonite (Na-B) and hybrid bentonites (50HDP-B, 100HDP-B, and 200HDP-B). [Colour online.]

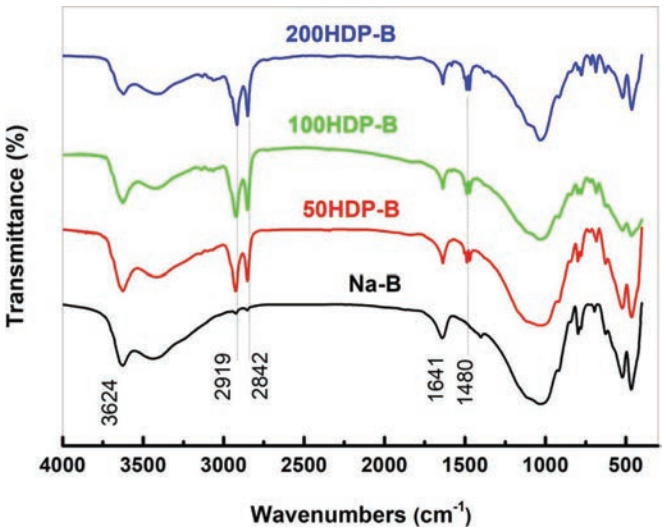

Adsorption kinetics

The effect of contact time on the adsorption of CR dye using sodic bentonite and synthesized organo-bentonites was examined in Fig. 2*a*. The adsorption yield of dye on adsorbent samples increases with the increase of contact time to reach a maximum sorption percentage at 60 min for Na-B and 200HDP-B. For the others (50HDP-B and 100HDP-B), the adsorption equilibrium was reached after 120 min of stirring.

Also, the rate of CR dye removal with modified bentonite adsorbents is primarily rapid in the first stages of contact time, and then, it is gradually slowed until reactions reach equilibrium. The rapid adsorption observed during the first stage of process was attributed to the abundance of free active sites on the HDP-B surface and easy availability of them for CR dye molecules.

As seen from Fig. 2*b*, the maximum percent removal adsorption at equilibrium time (t_e) of dye with pyridinium modified bentonite adsorbents 50HDP-B, 100HDP-B, and 200HDP-B was 72.1%, 96.1%, and 98.4%, respectively, whereas the adsorption yield of Na-B was 14.6%. It can be observed that the magnitudes of CR dye on all organo-modified bentonite are larger than that on Na-B, which can be ascribed to the hydrophobic effect and electrostatic attraction. This can be explained by the highly polar and hydrophilic of both the CR dye and modified bentonite. The intercalation of HDP onto bentonite not only provides a higher hydrophobicity to the adsorbent, but also changes the bentonite character from hydrophilic to hydrophobic, which enhances the electrostatic attraction between its surface and the dye molecules. This change is responsible for the improved adsorption efficiency observed in this study.[33,34]

As shown in Fig. 2*b*, CR dye adsorption on HDP-B increased with increasing pyridinium surfactant dose (%CEC) compared with only 7.37 mg g^{-1} adsorbed on Na-B, suggesting that the increase in HDP content significantly enhanced the removal rate of CR dye from solution. When the amounts of HDP on HDP-B increased from 50% to 100% of the CEC values, the adsorbed CR dye increased from 36.07 to 48.05 mg g^{-1}. However, when HDP increased to 200%, the amount of CR dye sorbed increased slightly to 49.21 mg g^{-1}, suggesting that HDP on the bentonite was overloaded when the pyridinium surfactant dose was over 100%. The organo-modified bentonites demonstrated higher adsorption efficiency compared with the unmodified bentonite. The high sorption capacity of CR

Fig. 2. (*a*) Kinetics curve of CR dye adsorption by using modified bentonites (HDP-B) and sodium bentonite (Na-B). pH = 6.6, C_0 = 50 mg L^{-1}, m/V = 1 g L^{-1}, T = 20 ± 1 °C. (*b*) The effect of pyridinium surfactant dose (% CEC) on the percent removal and equilibrium adsorption capacity of CR dye at t_e = 120 min. [Colour online.]

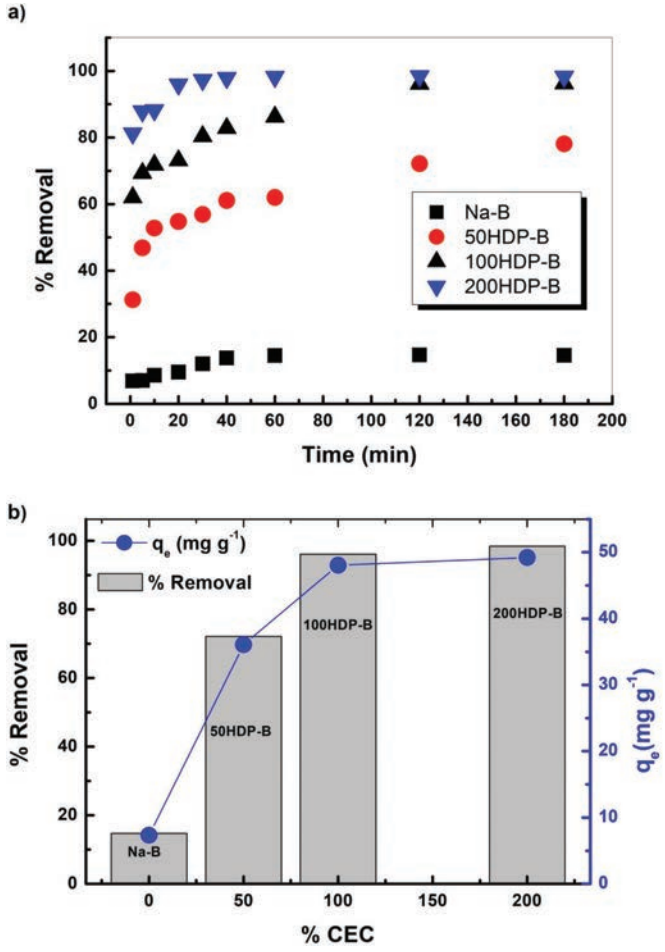

Fig. 3. Modeling of CR dye adsorption kinetics on Na-B and HDP-B samples. (*a*) pseudo first-order kinetic plot and (*b*) pseudo second-order kinetic plot. [Colour online.]

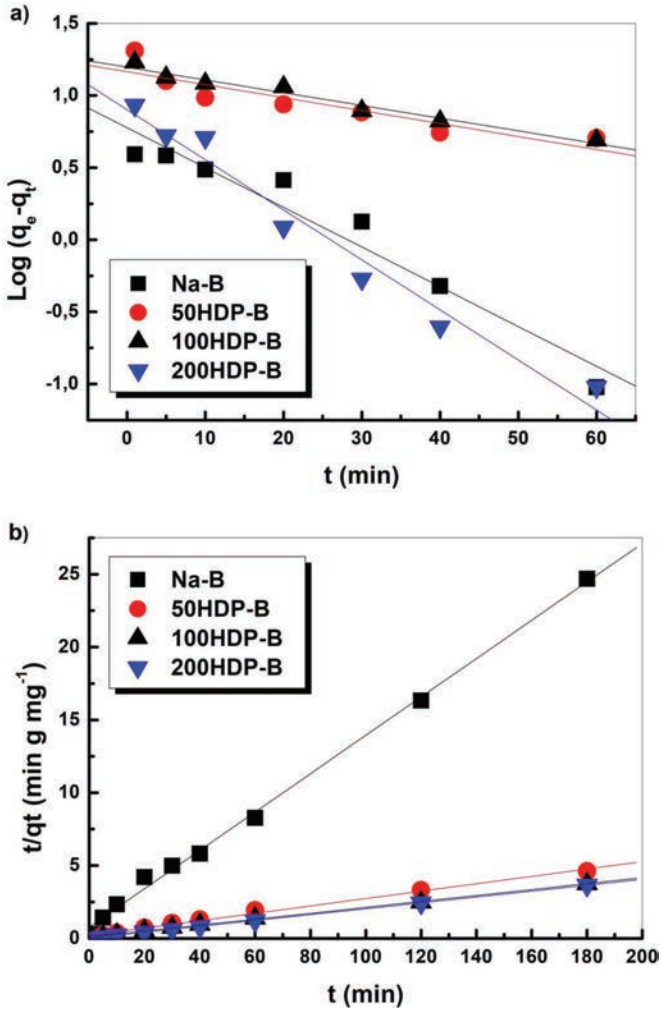

dye on hexadecylpyridinium modified bentonite adsorbents can be attributed to the high electrostatic attraction between the anionic SO_3^- group in CR dye and the positive head of the surfactant and (or) the van der Waals interaction between the dye molecules and surfactants.[35] Similar trends were reported by Xia et al.[36] in the adsorption of CR dye onto hectorite modified with cetyltrimethylammonium bromide and Li et al.[37] in the removal of Reactive Violet K-3R and Acid Dark Blue 2G onto cationic-polymer/bentonite.

The pseudo first-order and the pseudo second-order linear plots of CR dye adsorption kinetics data have been depicted in Fig. 3. Table 2 presents the results of the experimental data. It can be seen that the correlation coefficients (R^2 = 0.99) values are larger and the experimental values of adsorption capacity ($q_{e,exp}$) agreed with the calculated values ($q_{e,cal}$) in the pseudo second-order model. This indicates that the pseudo second-order model is the most suitable in describing the adsorption kinetics of CR dye on sodic bentonite and pyridinium-modified bentonites samples. The same result was found by Chitrakar et al.[38] in the adsorption of perchlorate ion onto montmorillonite modified with hexadecylpyridinium chloride and Zohra et al.[39] in the removal of Direct Red 2 on bentonite modified by cetyltrimethylammonium bromide.

Effect of adsorbent dosage (solid–solution ratio)

A comparison of Na-B and 100HDP-B on the CR dye adsorption at an initial dye concentration of 50 mg L^{-1} and an initial pH of 6.6 for different adsorbent dose intervals is depicted in Fig. 4*a*. The removal of anionic dye was low in the presence of sodic bentonite. However, it can be seen that the percent dye removal increased from 0.8% to 21.9% and 24.4% to 98.6% when the Na-B and 100HDP-B dosages were increased in the range of 0.1–2 g L^{-1}, respectively. The dye removal efficiency of the modified clay remains substantially constant at m/V ratios of ≥ 1 g L^{-1}. Such results clearly demonstrate the improved CR dye adsorption efficiency of bentonite after modification through the alkyl pyridinium surfactant.

Effect of initial dye concentration

The adsorption of CR dye by Na-B and 100HDP-B was investigated by varying its initial concentrations (50–500 mg L^{-1}) at the adsorbent dosage of 1 g L^{-1} and initial pH of 6.6 (Fig. 4*b*). For the 100HDP-B material, the yield is highest (96.1%) in initial dye concentrations ranging from 50 to 100 mg L^{-1} (appearance of a bearing). When the initial CR dye concentration was increased from 150 to 500 mg L^{-1}, the CR dye removal efficiency decreased from 91.9% to 54.6%. The reason for this result can be explained by the fact that the adsorbent has a limited number of active sites, which become saturated above a certain CR dye concentration. Similar observations were also reported in the literature for other adsorbates and different surfactant-modified clays.[40,41] For the Na-B adsorbent, low removals were obtained; the maximum is ob-

Table 2. Kinetic parameters for CR dye sorption.

			Pseudo first-order model			Pseudo second-order model			
Adsorbent	Removal	$q_{e,exp}$	k_1	$q_{e,cal}$	R^2	k_2 (×10³)	$q_{e,cal}$	R^2	h
Na-B	14.69	7.35	0.063	5.97	0.88	22.280	7.59	0.99	1.28
50HDP-B	72.13	36.07	0.020	14.64	0.67	3.217	39.42	0.99	4.99
100HDP-B	96.10	48.05	0.018	15.71	0.92	4.361	49.11	0.99	10.52
200HDP-B	98.43	49.21	0.080	7.98	0.92	37.934	49.38	0.99	92.50

Note: Removal (%), $q_{e,exp}$ (mg g^{-1}), $q_{e,cal}$ (mg g^{-1}), k_1 (min^{-1}), k_2 (g mg^{-1} min^{-1}), and h (mg g^{-1} min^{-1}).

Fig. 4. Effect of (*a*) adsorbent dosage and (*b*) initial dye concentration on the removal efficiency of CR dye.

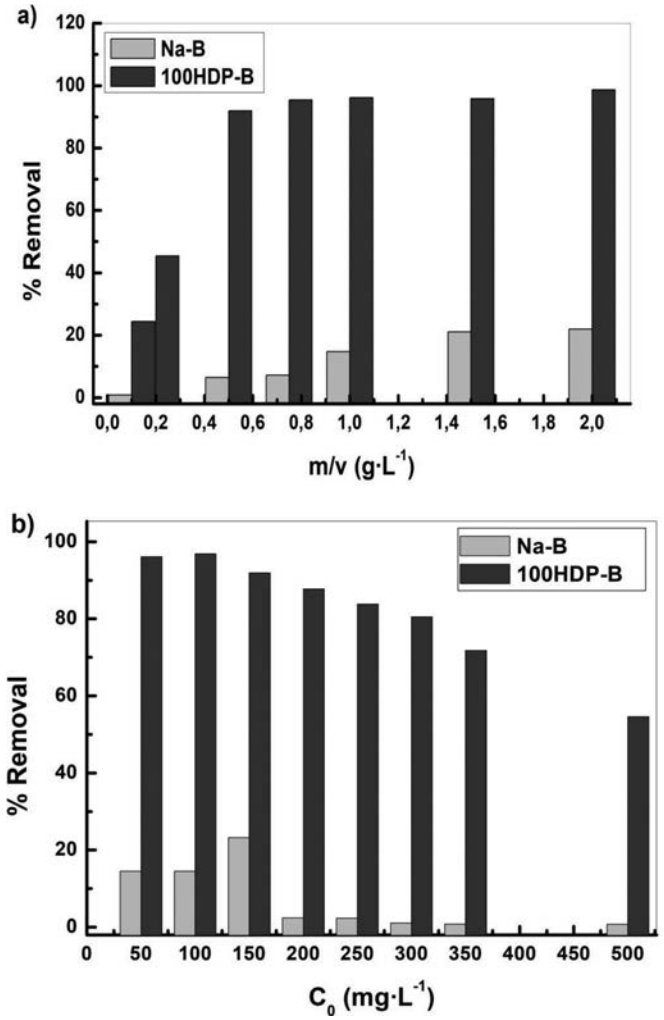

Table 3. Box–Behnken design matrix along with predicted and experimental values of percent removal of CR dye.

	Factor level			Removal (%)	
Run	X_1	X_2	X_3	Experimental	Predicted
1	–1	0	–1	95.11	96.21
2	–1	–1	0	40.56	34.39
3	–1	1	0	71.83	71.81
4	–1	0	1	37.69	42.78
5	0	1	–1	97.28	96.19
6	0	1	1	67.45	62.38
7	0	–1	1	23.83	24.91
8	0	–1	–1	60.64	65.71
9	1	0	–1	97.58	92.49
10	1	–1	0	50.23	50.25
11	1	0	1	72.42	71.32
12	1	1	0	74.60	80.77
13[a]	0	0	0	84.72	84.61
14[a]	0	0	0	85.28	84.61
15[a]	0	0	0	83.82	84.61

[a]Three additional tests at the central point (0, 0, 0) for the calculation of the Student and Fisher's tests.

Table 4. Statistical parameters of Box–Behnken design for the CR dye sorption process.

Term	Coefficient	Sum of squares	Df	Mean square	*F* ratio	*p* value
Constant	84.606	—	—	—	—	—
X_1:T	6.205	308.016	1	308.016	8.31	0.0345[a]
X_2:m/V	16.987	2308.6	1	2308.6	62.31	0.0005[a]
X_3:C_0	–18.652	2783.33	1	2783.33	75.13	0.0003[a]
X_1^2	–5.950	130.754	1	130.754	3.53	0.1191
X_1X_2	–1.725	11.9025	1	11.9025	0.32	0.5953
X_1X_3	8.065	260.177	1	260.177	7.02	0.0454[a]
X_2^2	–19.350	1382.6	1	1382.6	37.32	0.0017[a]
X_2X_3	1.745	12.1801	1	12.1801	0.33	0.5912
X_3^2	–2.955	32.2595	1	32.2595	0.87	0.3936
Total error		185.246	5	37.0492		
Total (correlation)		7330.94	14	308.016		

Note: df, degrees of freedom.
[a]Significant variable.

served at a concentration of 150 mg L^{-1} (23.2%), which then decreased to 0.8% when the initial concentration increased to 500 mg L^{-1}.

Effect of temperature

The effect of temperature on the adsorption of CR dye was examined at an initial concentration of 50 mg L^{-1} and m/V ratio of 1 g L^{-1}. It seems that the sorption process is affected within the range of 20–60 °C. The dye removal efficiency of CR increased slightly from 96.1% to 99.6% with increasing temperature from 20 to 60 °C, respectively. These results indicate the endothermic nature of the sorption process of the CR dye onto 100HDP-B.

Optimization of CR dye sorption process

The effect of process variables such as temperature, solid–solution ratio, and initial dye concentration on the sorption of CR dye onto 100HDP-B was investigated using response surface methodology according to Box–Behnken design. The codified values of three important factors (X_1, X_2, and X_3) together with their corresponding response values were listed in Table 3.

Multiple regression analysis of the experimental data yielded the following regression equation for the percent removal of CR dye. Table 4 shows the analysis of variance (ANOVA) model for the percent adsorption of dye using pyridinium-modified bentonite. ANOVA is required to test the significance and adequacy of the model.[42] This analysis makes it possible to test the relevance of the variables involved in the experimental design and graphically represent the importance of each parameter on the response obtained. The principle consists in comparing the variance of the experiments to evaluate whether they differ from the average or not. Then, it is necessary to compare the variance of various replicates of a sample with the variance of means between all sam-

Fig. 5. (*a*) Pareto chart of standardized effects, (*b*) comparison of predicted and observed percent removal of CR dye, and (*c*) surface plot of the percent removal of CR dye as a function of temperature and adsorbent dosage at the fixed initial dye concentration ($X_3 = 0$). [Colour online.]

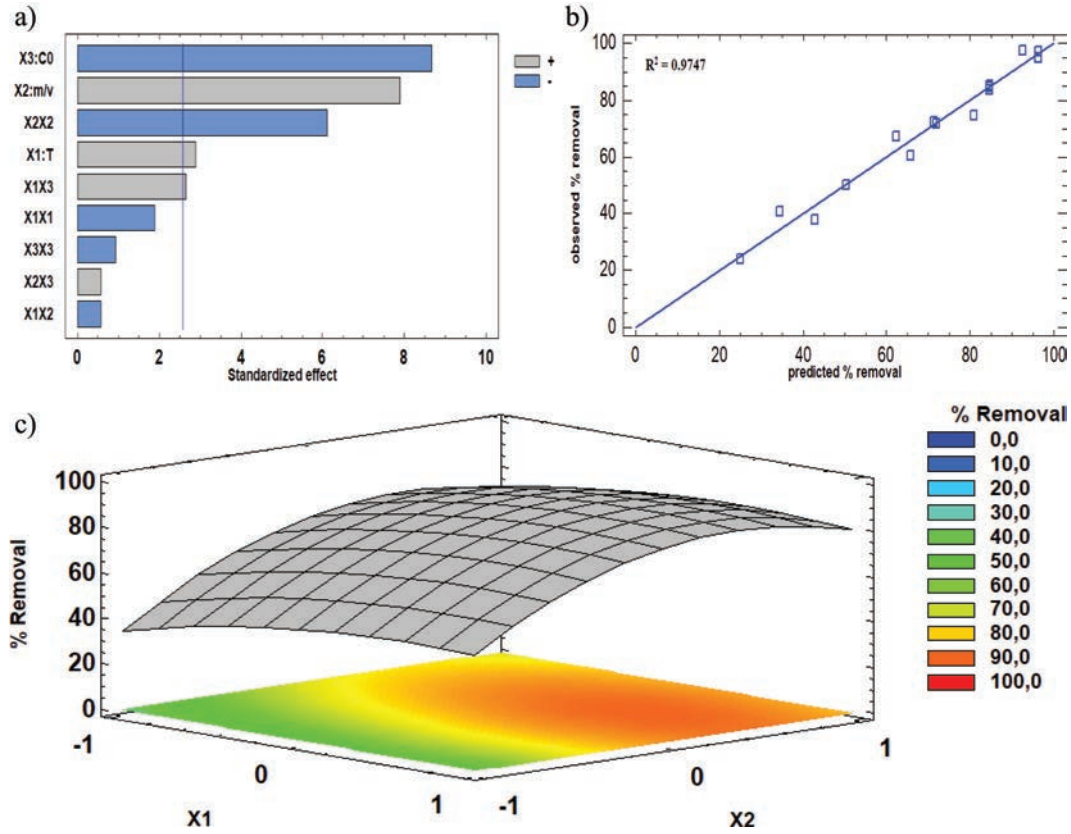

ples.[43] The relationship between these two variances is called the *F* ratio. The *F* ratio value depends on the number of degrees of freedom (df) involved in the model and represented in the *P* value column at a 95% confidence level by reference to a statistical table. As a result, effects less than 0.05 in this column are considered to be statistically significant. In this case, the linear effects of temperature, solid–solution ratio, and initial dye concentration are more significant. The square effects of adsorbent dosage and its interaction with temperature were also found to be statistically significant on the adsorption of CR dye onto 100HDP-B.

Following this statistical study, a Pareto chart diagram (Fig. 5*a*) representing the different effects in a standardized way could be drawn up to highlight the most significant effects in order of importance for each variable (linear, interaction, and quadratic effects). The crossbar represents the minimum amplitude at which the effects will be considered statistically significant for the response studied, considering a 95% confidence level. The interpretation of this chart demonstrates that the adsorbent dosage and initial dye concentration are highly significant. An increase in adsorbent dosage increases the sorption efficiency; however, the initial CR dye concentration has a net negative effect on percent removal. The interaction of temperature and initial dye concentration effect was very small in comparison with linear effects but it was also significant at a 95% confidence level. The lack of influence of cross-product effects (X_1X_2 and X_2X_3) suggests the weak influence of the interactions between the variables in the studied experimental domain. Moreover, the correlation coefficient (R^2 = 0.97) was very high, indicating a very good agreement between the observed results and predicted response, which shows good adaptation of the statistical model (Fig. 5*b*). After the elimination of the insignificant parameters ($p > 0.05$) and the substitution of the coefficients in eq. 7 with their values from Table 4, the best-fitting equation in terms of coded factors for CR dye adsorption was described as follows:

$$\text{(8)}\quad \%\ \text{removal} = 84.606 + 6.205X_1 + 16.987X_2 - 18.652X_3 + 8.065X_1X_3 - 19.350X_2^2$$

Response surface plots of the model were drawn to show the effect of the independent factors on the dependent factors. This was done by varying two factors within the experimental range and holding the other one constant. Figure 5*c* is the response surface plot showing the effect of temperature and solid–solution ratio on the CR dye removal at the fixed initial concentration of 275 mg L^{-1} ($X_3 = 0$). The polynomial equation of the second degree is also used to define optimal adsorption conditions. The mathematical equation was derived for each variable studied giving first-degree equations. The procedure involves equalizing the derivatives to 0 and solving the equation to give optimal conditions in coded values. These values are then decoded, based on the experience plan in real values. The optimal values of the parameters affecting the quantitative adsorption were calculated and are 44 °C for the temperature, 0.74 g L^{-1} for the adsorbent dosage, and 100 mg L^{-1} for the initial dye concentration. All of these optimal values are within the experimental range of factors considered in this study.

Conclusion

As a result, the kinetics and optimization process indicate that the modified bentonite at different amounts of a surfactant allows us to increase the adsorption capacity. The series of modified bentonite were successfully prepared using the intercalated process. The adsorbed amounts of CR dye on modified bentonite

with HDP of different surfactant doses (50HDP-B, 100HDP-B, and 200HDP-B) are considerably higher than that on Na-B. Kinetic studies indicated that the adsorption of CR dye onto HDP-B adsorbents or Na-B was found to follow the pseudo second-order reaction. Response surface methodology with three-variable, three-level Box–Behnken design of utmost importance to reduce the number of experiment variables and provide useful information about the effect of the factors and their possible interactions, as well as to optimize the conditions for dye treatment. The effect of three variables such as temperature, adsorbent dosage, and initial dye concentration onto 100HDP-B from aqueous solutions was studied. The statistical analysis confirmed that the dye removal efficiency was enhanced by an increase in adsorbent dosage and temperature and a decrease in initial dye concentration. It is also observed that the interactive effect of temperature and initial dye concentration, as well as the square effect of adsorbent dosage, were found to have a significant influence on dye adsorption. The optimum values of temperature, adsorbent dosage, and initial dye concentration were found to be 44 °C, 0.74 g L^{-1}, and 100 mg L^{-1} for the complete removal of CR dye, respectively. The present results show that modified bentonite with the HDP is a promising adsorbent for removing CR dye from aqueous solution.

Acknowledgements

We gratefully acknowledge the ATRST (Agence Thématique de Recherche en Sciences & Technologie-Algérie) (ex. ANDRU) for their financial support.

References

(1) Pearce, C.; Lloyd, J.; Guthrie, J. *Dyes Pigments* **2003**, *58*, 179. doi:10.1016/S0143-7208(03)00064-0.
(2) Zollinger, V. H. Colour chemistry. Synthesis, properties and applications of organic dyes and pigments. 1987, 92.
(3) Robert, D.; Parra, S.; Pulgarin, C.; Krzton, A.; Weber, J. V. *Appl. Surf. Sci.* **2000**, *167*, 51. doi:10.1016/S0169-4332(00)00496-7.
(4) Guillard, C.; Lachheb, H.; Houas, A.; Ksibi, M.; Elaloui, E.; Herrmann, J.-M. *J. Photochem. Photobiol. A Chem.* **2003**, *158*, 27. doi:10.1016/S1010-6030(03)00016-9.
(5) Pandey, A.; Singh, P.; Iyengar, L. *Int. Biodeterior. Biodegrad.* **2007**, *59*, 73. doi:10.1016/j.ibiod.2006.08.006.
(6) Bauer, C.; Jacques, P.; Kalt, A. *J. Photochem. Photobiol. A Chem.* **2001**, *140*, 87. doi:10.1016/S1010-6030(01)00391-4.
(7) Brown, M. A.; De Vito, S. C. *Crit. Rev. Environ. Sci. Technol.* **1993**, *23*, 249. doi:10.1080/10643389309388453.
(8) Balakrishnan, V. K.; Palabrica, V. *Can. J. Chem.* **2010**, *88* (4), 393. doi:10.1139/V10-018.
(9) Pagga, U.; Brown, D. *Chemosphere* **1986**, *15*, 479. doi:10.1016/0045-6535(86)90542-4.
(10) Chakraborty, A.; Acharya, H. *Colloid Interface Sci. Commun.* **2018**, *24*, 35. doi:10.1016/j.colcom.2018.03.005.
(11) Zhao, W.; Wu, Z.; Wang, D. *J. Hazard. Mater.* **2006**, *137*, 1859. doi:10.1016/j.jhazmat.2006.05.032.
(12) Liu, S.; Li, B.; Qi, P.; Yu, W.; Zhao, J.; Liu, Y. *Colloid Interface Sci. Commun.* **2019**, *28*, 34. doi:10.1016/j.colcom.2018.11.004.
(13) Ciardelli, G.; Corsi, L.; Marcucci, M. *Resour. Conserv. Recycl.* **2001**, *31*, 189. doi:10.1016/S0921-3449(00)00079-3.
(14) Arslan, I.; Balcioğlu, I. A. *Dyes Pigments* **1999**, *43*, 95. doi:10.1016/S0143-7208(99)00048-0.
(15) Dinesh, G. K.; Saranya, R. *Can. J. Chem.* **2018**, *96* (10), 897. doi:10.1139/cjc-2017-0696.
(16) Kornaros, M.; Lyberatos, G. *J. Hazard. Mater.* **2006**, *136*, 95. doi:10.1016/j.jhazmat.2005.11.018.
(17) Khan, S.; Malik, A. *Can. J. Microbiol.* **2016**, *62* (3), 220. doi:10.1139/cjm-2015-0552.
(18) Vimonses, V.; Lei, S.; Jin, B.; Chow, C. W.; Saint, C. *Chem. Eng. J.* **2009**, *148*, 354. doi:10.1016/j.cej.2008.09.009.
(19) Hao, T.; Rao, X.; Li, Z.; Niu, C.; Wang, J.; Su, X. *J. Alloys Compd.* **2014**, *617*, 76. doi:10.1016/j.jallcom.2014.07.111.
(20) Pal, S.; Patra, A. S.; Ghorai, S.; Sarkar, A. K.; Mahato, V.; Sarkar, S.; Singh, R. *Bioresour. Technol.* **2015**, *191*, 291. doi:10.1016/j.biortech.2015.04.099.
(21) Shu, J.; Wang, Z.; Huang, Y.; Huang, N.; Ren, C.; Zhang, W. *J. Alloys Compd.* **2015**, *633*, 338. doi:10.1016/j.jallcom.2015.02.048.
(22) Makhoukhi, B.; Didi, M. A.; Villemin, D. *Mater. Lett.* **2008**, *62*, 2493. doi:10.1016/j.matlet.2007.12.026.
(23) Makhoukhi, B.; Djab, M.; Didi, M. A. *J. Environ. Chem. Eng.* **2015**, *3*, 1384. doi:10.1016/j.jece.2014.12.012.
(24) Arab, P. B.; Araújo, T. P.; Pejon, O. J. *Appl. Clay Sci.* **2015**, *114*, 133. doi:10.1016/j.clay.2015.05.020.
(25) Baskaralingam, P.; Pulikesi, M.; Elango, D.; Ramamurthi, V.; Sivanesan, S. *J. Hazard. Mater.* **2006**, *128*, 138. doi:10.1016/j.jhazmat.2005.07.049.
(26) Ho, Y.; McKay, G. *J. Environ. Sci. Health, Part A: Toxic/Hazard. Subst. Environ. Eng.* **1999**, *34*, 1179. doi:10.1080/10934529909376889.
(27) Ho, Y.-S.; McKay, G. *Water Res.* **2000**, *34*, 735. doi:10.1016/S0043-1354(99)00232-8.
(28) Mishra, A. K.; Allauddin, S.; Narayan, R.; Aminabhavi, T. M.; Raju, K. *Ceram. Int.* **2012**, *38*, 929. doi:10.1016/j.ceramint.2011.08.012.
(29) Ma, Y.; Zhu, J.; He, H.; Yuan, P.; Shen, W.; Liu, D. *Spectrochim. Acta, Part A,* **2010**, *76*, 122. doi:10.1016/j.saa.2010.02.038.
(30) Madejova, J. *Vib. Spectrosc.* **2003**, *31*, 1. doi:10.1016/S0924-2031(02)00065-6.
(31) Xia, M.; Jiang, Y.; Li, F.; Sun, M.; Xue, B.; Chen, X. *Colloids Surf., A* **2009**, *338*, 1. doi:10.1016/j.colsurfa.2008.12.043.
(32) Gammoudi, S.; Frini-Srasra, N.; Srasra, E. *Engi. Geol.* **2012**, *124*, 119. doi:10.1016/j.enggeo.2011.10.009.
(33) Andrzejewska, A.; Krysztafkiewicz, A.; Jesionowski, T. *Dyes Pigments* **2007**, *75*, 116. doi:10.1016/j.dyepig.2006.05.027.
(34) de Farias, R. S.; de Brito Buarque, H. L.; da Cruz, M. R.; Cardoso, L. M. F.; de Aquino Gondim, T.; de Paulo, V. R. *Eng. Sanit. Ambiental* **2018**, *23*, 1053. doi:10.1590/s1413-41522018172982.
(35) Foroughi-dahr, M.; Abolghasemi, H.; Esmaieli, M.; Nazari, G.; Rasem, B. *Process Saf. Environ. Prot.* **2015**, *95*, 226. doi:10.1016/j.psep.2015.03.005.
(36) Xia, C.; Jing, Y.; Jia, Y.; Yue, D.; Ma, J.; Yin, X. *Desalination* **2011**, *265*, 81. doi:10.1016/j.desal.2010.07.035.
(37) Li, Q.; Yue, Q.-Y.; Sun, H.-J.; Su, Y.; Gao, B.-Y. *J. Environ. Manage.* **2010**, *91*, 1601. doi:10.1016/j.jenvman.2010.03.001.
(38) Chitrakar, R.; Makita, Y.; Hirotsu, T.; Sonoda, A. *Chem. Eng. J.* **2012**, *191*, 141. doi:10.1016/j.cej.2012.02.085.
(39) Zohra, B.; Aicha, K.; Fatima, S.; Nourredine, B.; Zoubir, D. *Chem. Eng. J.* **2008**, *136*, 295. doi:10.1016/j.cej.2007.03.086.
(40) Shirzad-Siboni, M.; Khataee, A.; Hassani, A.; Karaca, S. *C. R. Chim.* **2015**, *18*, 204. doi:10.1016/j.crci.2014.06.004.
(41) Toor, M.; Jin, B. *Chem. Eng. J.* **2012**, *187*, 79. doi:10.1016/j.cej.2012.01.089.
(42) Rajasimman, M.; Sangeetha, R.; Karthik, P. *Chem. Eng. J.* **2009**, *150*, 275. doi:10.1016/j.cej.2008.12.026.
(43) Lazic, Z. R. Design of experiments in chemical engineering: a practical guide. John Wiley & Sons, 2006.